Implementation of system identification and flight control system for UAV

Conference Paper · April 2017

DOI: 10.1109/ICCAR.2017.7942783

4 authors:

Watcharapol Saengphet
Suranaree University of Technology

Suradet Tantrairatn
Suranaree University of Technology

Chalothorn Thumthae
Suranaree University of Technology

Jiraphon Srisertpol
Suranaree University of Technology

Implementation of System Identification and Flight Control System for UAV

Watcharapol Saengphet, Suradet Tantrairatn, Chalothorn Thumtae, Jiraphon Srisertpol
School of Mechanical Engineering
Suranaree University of Technology
Nakhon Ratchasima, Thailand
e-mail: w.saengphet@hotmail.com, suradetj@sut.ac.th, chalothorn@sut.ac.th, jiraphon@sut.ac.th

***Abstract*—This paper presents a methodology to implement a flight control system based on PID control design for PX4 autopilot system. The objective of the method is to find out the optimal controller gains on the same control structure of PX4 flight stack software without iterative controller tuning. This is achieved through a two-step procedure which consist of aircraft system identification and PID optimized control design. The first step to implement an autopilot system on an Unmanned Aerial Vehicle (UAV) relates to characterizing the UAV's dynamics using a mathematical model. To accomplish the accuracy of the particular UAV control, the process of system identification, which is the estimation of the parameters of the equation of motion, is essential. The measurement of inputs and outputs during manual flight is utilized to determine the unknown parameters of SISO mathematical model using a software of comprehensive identification from frequency responses. Subsequently, the model is utilized for an optimization-based tuning of these PID controller gains offline in order to minimize the requirement of numerous in-flight tuning. The controller is implemented on PX4 autopilot system. The results are demonstrated that the tracking control system has excellent dynamic performance in respect of simple design, high precision, and easy implement.**

Keywords-flight control system; UAV control; system identification

I. INTRODUCTION

Unmanned Aerial Vehicles (UAVs) have been widely used and become very popular application for Traffic monitoring [1] reconnaissance and surveillance [2]. Low-cost commercial flight controllers that already integrated the important sensors for UAV are available such as APM [3] and Pixhawk [4]. Furthermore, there are some open source flight control software, for example, PX4 [5] that use PID controller. PID control technique is a popular method due to its past record of wide availability and simplicity of use.

The heuristic tuning approach can be applied for PI or PID controller. Ziegler-Nichols method is the most popular. Since controller gain can be tuned without aircraft dynamic model. Other method such as Tyreus- Luyben tuning and Astrom-Hagglund tuning methods can be applied [6].

Reference [7] designed UAV flight stabilization system for longitudinal and lateral axis of Cessna 172 model. MATLAB/Simulink and Xplane were utilized to design PID controller and Hardware-In-the-Loop (HIL) simulation.

However, without a model, controller gain tuning requires an iterative process. Therefore, the flight should be conducted by an experienced pilot in order to avoid the chance of pilot error and to reduce the number of iterations. Therefore, controller tuning technique, which relies on dynamic model, is interesting if the system identification process in order to obtain dynamic model is not too complicated.

MATLAB offers the Control System Designer [8]. Simulink linearized the control block around the trimmed point or initial condition. Local and global optimization method are based on a gradient descent and pattern search such as Genetic Algorithm (GA), respectively.

Control System Designer tool is utilized [9] to optimized the lead compensator for altitude acquire and hold. The hybrid approach was employed, which to find feasible solution with any global method and then to get optimum solution with local method in order to meet the best approach to find optimum solution for such multimodal functions.

An UAV's dynamic model can be determined from flight data, after which the dynamic model can be used to develop and validate autopilot control systems. Thus system identification is a tool for modeling, and developing controllers for aircraft dynamics. System identification provides a base for reliable and robust UAV control systems resulting in higher success rates and safety [10].

Many system ID methods have seen successfully applied to small low-cost UAV [10]. Tischler developed the software package Comprehensive Identification from Frequency Responses (CIFER) [11]. This software has been applied to helicopter UAVs [12]. Although CIFER is mainly used for helicopter, many literatures have shown that the software can also be applied for the fixed-wing UAV [13]-[14].

This paper presents identification results of the Tailless UAV, deriving two linear SISO models, one for the longitudinal dynamics using the elevator command as input and the pitch angular rate as output, and the other for lateral dynamics using the aileron command as input and the roll angular rate as output. In section II a short description of the Tailless UAV, the hardware and software used in the experiments is given. System ID method using the frequency domain identification approach for this research is presented in Section III. Optimization controller gained by MATLAB/Simulink is explained in Section IV. Results of the ID both pitch and roll response are presented in

978-1-5090-6088-7/17/$31.00

section V. Optimization result and flight test results are compared and discussed in Section VI.

II. General UAV Model and Flight Control

A. Gerneral UAV Model

UAV model is a tailless or flying wing aircraft. Since there is an unconventional platform, elevons are used to control the attitude for both pitch and roll maneuver. Elevons receives a mixed signal between elevator and aileron command from flight control system. The default of attitude controller gains does not provide suitable value for this platform. Therefore, it must be tuned before performing the automatic flight mode such as stabilizing and loitering. Table I shows the important parameters of the UAV.

B. Hardware

The Pixhawk board which contains an advanced 32-bit ARM Cortex® M4 Processor running NuttX real-time operating system (RTOS) was selected as an autopilot hardware for validation. There are 14 PWM servo outputs and a number of communication interfaces, such as serial ports, I2C and SPI. Furthermore, the Pixhawk is integrated with compass, accelerometer and gyroscope, GPS, etc. [4]. The onboard sensors of the Pixhawk comprise dual IMU for additional redundancy and accuracy of measurements. The Pixhawk also features an SD card slot for storage of flight data logs. User is able to set the desired sample rate.

TABLE I. Tialless UAV Parameters

Span	1.2 m	**Sweep angle**	30 degree
Chord	0.16 m	**Motor**	Brushless
Length	0.45 m	**Flight time**	15 minutes
Control	Elevon	**Speed**	10-25 m/s
Weight	850 g	**Battery**	LiPo-3000 mAh
Airfoil	Epler 340	**Board**	Pixhawk 2.4.8

Figure 1. Tailless UAV model (left) and Pixhawk flight controller (right)

C. Software

PX4 flight stack [6] is used as autopilot software. The wing flight controller is based on feedback control, Proportional-Integral (PI), and feedforward control (FF) as shown in Fig. 1. PX4 scaled the PI and FF gain about the trimmed airspeed to decrease oscillation when the UAV fly too far from trimmed airspeed. In this research, airspeed scaler is assumed as constant.

Pitch and roll controller share the same structure. Angle error is converted to angular rate set-point by multiplied Time constant (T_c). Its value is 0.4 s as default. The angular rate set-point is converted to actuator control signal by multiplied feedforward gain. This signal is added by PI signal which is converted from the angular rate error. Controller gain PI and FF must be optimized to meet a required control performance in order to satisfy flying quality.

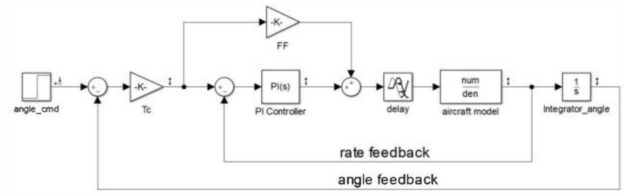

Figure 2. PX4 fixed wing controller block diagram

III. System Identification

Since PX4 fixed wing flight controller is a single input single output system (SISO). Decoupling between longitudinal and lateral dynamic are assumed. Therefore, the attitude controller gains can be tuned separately after obtaining the transfer function model of each axis. Next section explained the system identification method.

In order to obtain the desired frequency spectrum, the elevator and aileron command were programmed into the board based on PX4 flight stack. Automated frequency sweep was generated. The exponentially increasing sweep frequency is used to ensure that more time is spent on the lower frequencies and less time as on the higher frequencies. The values of sweep parameters depend on frequency range of interest as shown in Table II. The following equations were programmed to generate sweep signal.

$$\delta_{sweep} = A\sin[\theta(t)] \tag{1}$$

$$\theta(t) = \int_0^{T_{rec}} \omega(t)dt \tag{2}$$

$$\omega = \omega_{\min} + K(\omega_{\max} - \omega_{\min}) \tag{3}$$

$$K = C_2[\exp((C_1 t)/T_{rec}) - 1] \tag{4}$$

$$C_1 = 4.0 \text{ and } C_2 = 0.0187 \tag{5}$$

The sweep data were processed using CIFER to generate the frequency response. The frequency response is obtained from FRESPID tool in CIFER that uses a chirp z-transform. For the longitudinal and lateral dynamic model, input is at control command started from 0 which is trimmed condition and output is pitch or roll rate. Results from FRESPID are passed onto COMPOSITE to achieve the final frequency response database with excellent resolution and low random error [10]. Coherence more than 0.6 is acceptable [10]. Transfer function model was identified using NAVFIT. The model based on Low Order Equivalent System (LOES). LOES model is the same as classical dynamic modes, except for the inputs which are control command with equivalent time delays, instead of control surface deflections [15]. Eq. 6 was for both roll and pitch response.

$$\frac{q}{\eta_e} = \frac{(b_1 s + b_0) \cdot e^{-\tau_e s}}{s^2 + a_1 s + a_0} \quad (6)$$

The data was collected by flying the aircraft and measuring responses to elevator and aileron commands and recorded on SD card. Minimum and maximum sweep frequency were selected from typical pilot control input for fixed wing UAV.

TABLE II. COMPUTER-GENERATED SWEEP PARAMETERS

Parameter		Pitch	Roll
Sweep amplitude	A	0.2	0.15
Minimum frequency	$\omega_{\min}$	0.4 Hz	0.4 Hz
Minimum frequency	$\omega_{\max}$	6 Hz	6 Hz
Sweep record length	t_{rec}	13	13

IV. OPTTIMIZATION BASED TUNNING

MATLAB offers control system designer application to design or optimize the controller gain to meet the requirement. The gradient descent was selected as the optimization method by the default to minimize the objective function. Although it is a local method, if the result shown reasonable value, it would be applicable. However, if it is not, the global method, genetic algorithm, would be used instead [9]. All tolerance was set to 10^{-6}. Table III and IV shown the requirements and bound of attitude controller gain.

Since gradient descent method is a local optimization, the initial condition is very important. Therefore, the initial guess value, minimum and maximum value in Table IV are obtained from PX4 code, fixed wing attitude controller.

TABLE III. OPTIMIZATION REQUIREMENTS

Constraints	Pitch	Roll
Rise time (s)	1.25	0.3
% Rise	80	80
Settling time (s)	4.25	1.2
% Settling	3	3
% Overshoot	10	10
GM (dB)	> 5	> 5
PM (deg)	> 60	> 60

TABLE IV. CONTROLLER GAIN BOUNDS

Parameter	Initial guess		min	Max
	Pitch	Roll		
P	0.08	0.05	0.005	1
I	0.02	0.01	0.005	0.5
FF	0.5	0.5	0	1

V. SYSTEM IDENTIFICATION RESULT

The pitch and roll rate are in deg/s. In the interested frequency range, approximately 3-40 rad/s, coherence both pitch and roll response are greater than 0.6 and close to 1 (ideal). The second order model with time delay is enough to fit the frequency response. The system identification results are shown as Fig. 3 to Fig. 12 which are pitch rate, bode plot, time domain verification, transfer function model, and root locus plot.

A. Pitch Response

High frequency amplified the pitch rate magnitude and attenuated it after 20 rad/s. The phase started around -180 degree because the positive signal command produced the negative response such as pitch down or roll left. However, the experimental result shown phase-lag (phase lower than -180 degree). To reduce the cost function in order to improve the model precision, equivalent time delay was used to account for the phase-lag effects caused by unmodeled high-frequency dynamics.

The open loop transfer function of pitch response is shown as Eq. 7. The root locus plot (Fig. 7) indicated that the system is stable. Damping ratio is 0.34 at 20.4 rad/s. However, it is possible to reach the instability. Therefore, this model would be used to tune the controller gain carefully in the attitude controller optimization section.

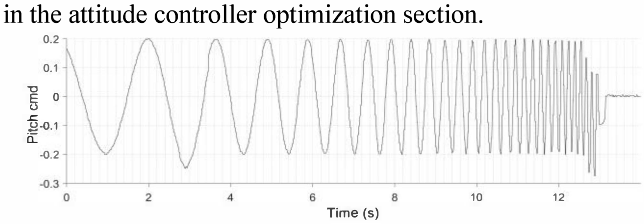

Figure 3. Elevator sweep command

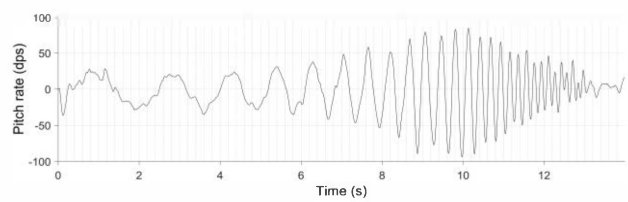

Figure 4. Pitch rate (deg/s)

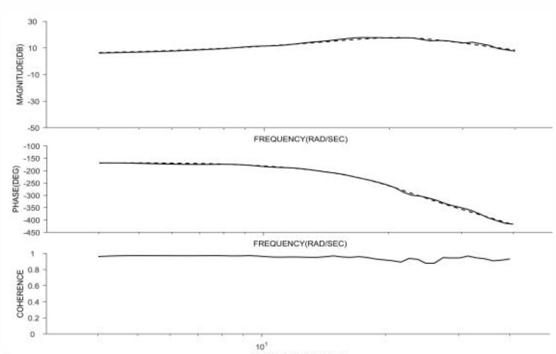

Figure 5. Bode plot for experimental result and pitch transfer function

$$\frac{q}{\eta_e} = \frac{(-106.2s + 677) \cdot e^{-0.0632s}}{s^2 + 13.69s + 416.7} \tag{7}$$

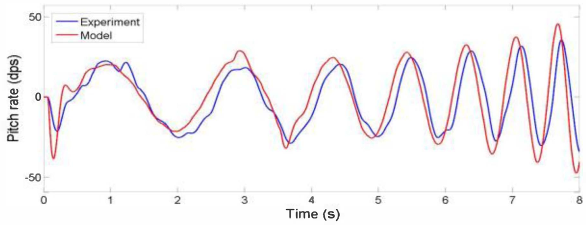

Figure 6. Time domain verification of elevator command to pitch rate

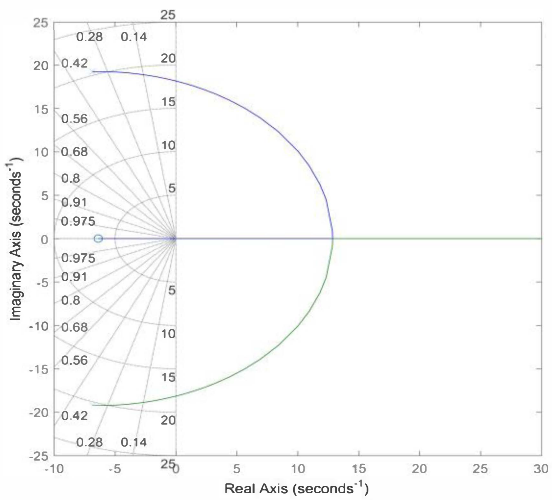

Figure 7. Root locus plot of the open loop pitch rate and pitch command

B. Roll Response

There is a difference between roll and pitch response. High frequency did not amplify or attenuate the roll rate magnitude. However, the phase-lag of roll response is lower than pitch response in comparison to the same frequency.

The open loop transfer function of roll response is shown as Eq. 8. The root locus plot (Fig. 12) indicated that the system is stable. The characteristic root laid on the real axis. Roll response is more stable than pitch response.

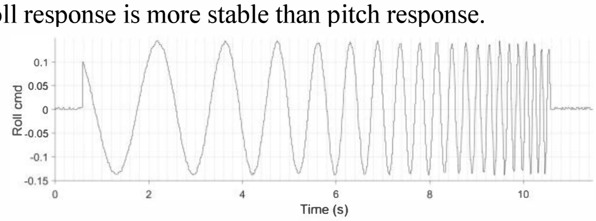

Figure 8. Aileron sweep command

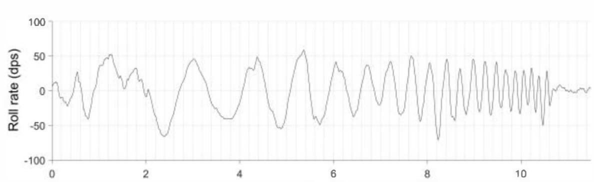

Figure 9. Roll rate (deg/s)

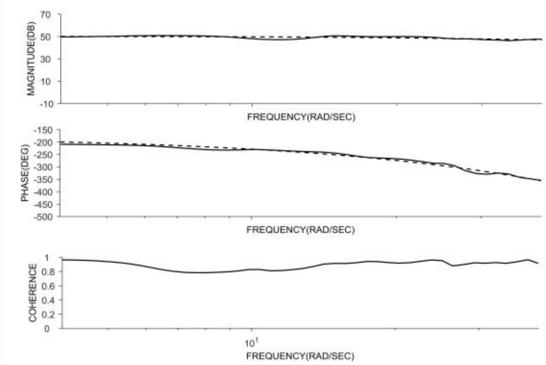

Figure 10. Bode plot for experimental result and roll transfer function

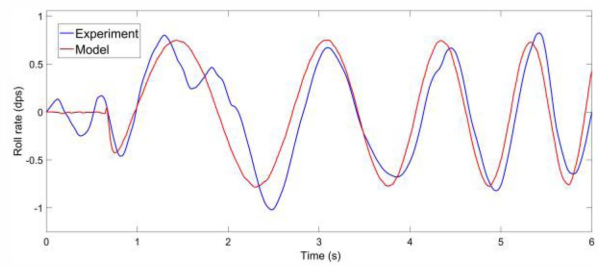

Figure 11. Time domain verification of aileron command to roll rate

$$\frac{q}{\eta_e} = \frac{(302.8s + 18510) \cdot e^{-0.0299s}}{s^2 + 136.5s + 3353} \tag{8}$$

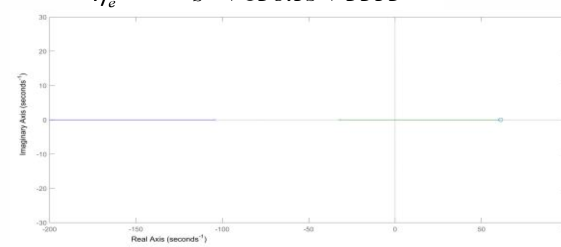

Figure 12. Root locus plot of the open loop roll rate and pitch command

VI. Attitude Controller Gain Tunning Result

A. Optimization Result

The desired reference signal and constraints implemented in the Simulink Signal Constraint Block (SCB) appear in Fig. 13 to Fig. 16. The white area in these figure shows the feasible region for these problems. No overshoot appeared in pitch response. Small overshoot appeared in roll response within the white area.

Since the gradient descent is a local optimization, the initial guess was set to 3 types as in table V. The RUN 1 value obtained from default. The RUN 2 and RUN 3 decrease and increase the P and I gain by double. The result shown that 3 runs have different value. However, there are not much different, especially for the P gain.

For the requirement of pitch response, the optimization was done successfully. The rise time is 1.25 s. Overshoot occurred which is acceptable. Gain margin is 5.7 dB at 20.7 rad/s. The close loop control is stable. However, if the rise time was set lower than 1.25 s, the optimization could not reach the gain margin requirement (lower than 5 dB) which leads the pitch stability to be unstable. However, if the rise time was too large, the aircraft could not track the angle set-point especially under the disturbance, gust wind. The selected rise time will be validated during the flight test.

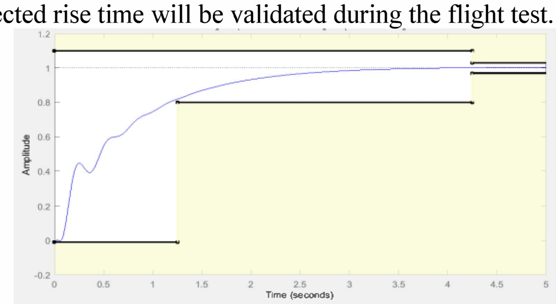

Figure 13. Pitch response and constraints in Simulink SCB

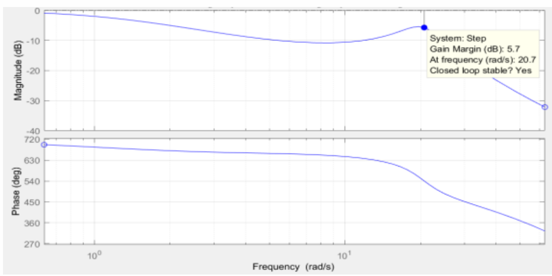

Figure 14. Bode plot of pitch response and constraints in Simulink SCB

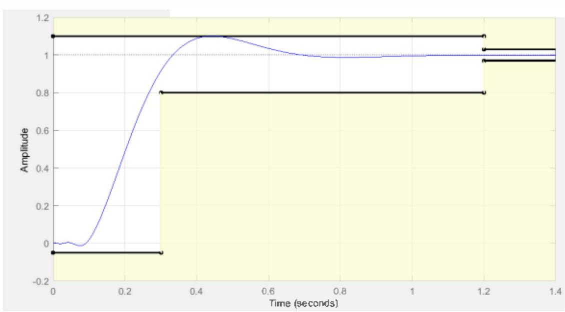

Figure 15. Roll response signal and constraints in Simulink SCB

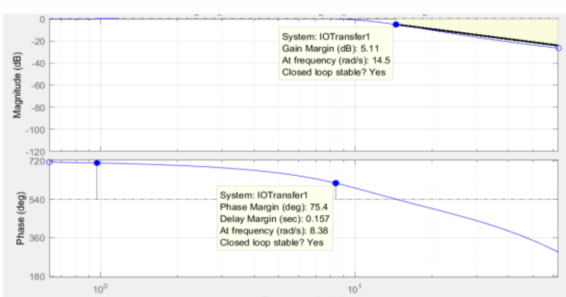

Figure 16. Bode plot of roll response and constraints in Simulink SCB

For the roll response, rise time is 0.3 s. The optimization succeeds in this requirement. However, if rise time was set to 0.2 s, the optimization will not succeed unless the gain margin. Therefore, the stability decreased. Roll angle time response (Fig. 15) indicated that the overshoot is 10%. However, this value stays within the requirement bound. The bode plot of roll angle response (Fig. 16) shown that gain margin is 5.11 dB at 14.5 rad/s, phase margin is 75.4 degree at 8.38 rad/s.

TABLE V. PITCH CONTROLLER GAIN

Parameter	RUN 1	RUN 2	RUN 3
Guess [P I FF]	[0.08 0.02 0.5]	[0.04 0.01 0.25]	[0.16 0.04 0.5]
Eval-Count	28	28	70
Number of iter	1	1	4
Result [P I FF]	[0.01 0.005 0.361]	[0.01 0.005 0.353]	[0.01 0.01 0.356]

TABLE VI. ROLL CONTROLLER GAIN

Parameter	RUN 1	RUN 2	RUN 3
Guess [P I FF]	[0.05 0.01 0.5]	[0.025 0.005 0.5]	[0.1 0.02 0.5]
Eval-Count	33	33	33
Number of iter	2	2	2
Result [P I FF]	[0.02 0.006 0.40]	[0.02 0.005 0.40]	[0.019 0.015 0.40]

TABLE VII. ATTITUDE CONROLLER GAIN DURING FLIGHT TEST

Parameter	Pitch	Roll
P	0.01 (0.02)	0.02 (0.02)
I	0.01 (0.02)	0.01 (0.02)
FF	0.36 (0.4)	0.40 (0.42)

Note that in the parentheses are manually tuned gain value.

B. Flight Test and Discussion

The optimized controller gains were put into the flight controller board for flight test. The tailless UAV was flown among the average wind speed of 3 m/s and maximum speed of 5.5 m/s.

Fig. 17 shown the pitch response of the default controller gain. The result indicated that the controller gain is not suitable for this UAV as the large pitch oscillation about the set-point occurred. The optimized controller gains as shown in table VII were used instead.

The optimized controller gains that are close to manually tuned controller gains shown satisfactory results. The UAV can track both pitch and roll angle set-point as shown in Fig 18 and Fig. 19. The controller tried to reject disturbance, gust wind. Therefore, the small amplitude and period of oscillation were resulted from gust wind. However, it is acceptable because it has not significantly affect the flying quality and the UAV is controllable.

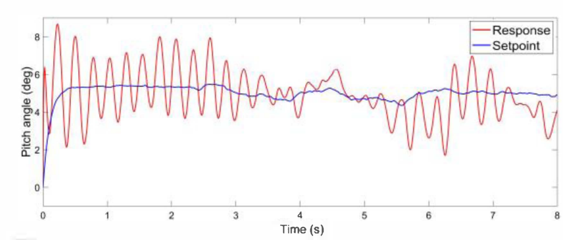

Figure 17. Pitch angle response for the default controller gain

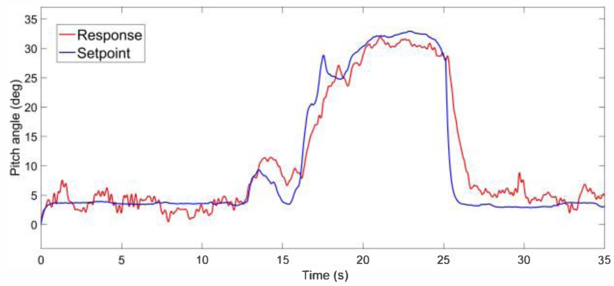

Figure 18. Pitch angle response for the optimized controller gain

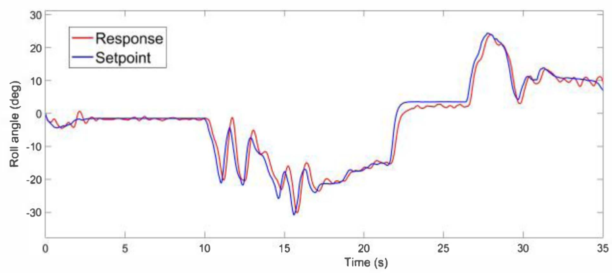

Figure 19. Roll angle response for the optimized controller gain

VII. CONCLUSION AND FUTURE WORK

This paper presented the controller tuning technique based on using a transfer function obtained from system identification. The PID controller gains are achieved by the optimization on MATLAB control system designer toolbox. The flight results shown excellent result that can track the set-point/command and reject the disturbance along with numerous benefits such as deceasing time consuming during the controller gain tuning and reducing the chance from pilot error due to repetition. Moreover, the frequency response obtained during the system identification process can also be used for the handling quality providing the opportunity for the designer to evaluate the UAV according to design, test, and evaluation procedure and to improve the pilot and flight controller performance and safety. If the proper mathematical model was used, the important parameters could be extracted and would be compared to the design value.

REFERENCES

[1] H.C.M. Veerman B.Sc. Preliminary Multi-Mission UAS Design. M.S. thesis, Delft University of Technology, Netherland, 2012.

[2] Spyridon G. Kontogiannis and John A. Ekaterinaris, "Design, performance evaluation and optimization of a UAV," Aerospace Science and Technology, vol.29, April 2013, pp. 339–350, doi: 10.1016/j.ast.2013.04.005.

[3] [Online] Available at: http://ardupilot.org/plane/docs/common-apm25-and-26-overview.html#common-apm25-and-26-overview [Accessed 19 Jan. 2017].

[4] [Online] Available at: https://pixhawk.org/ [Accessed 19 Jan. 2017].

[5] [Online] Available at: https://dev.px4.io/ [Accessed 19 Jan. 2017].

[6] G. Sudha and S. N. Deepa, "Optimization for PID Control Parameters on Pitch Control of Aircraft Dynamics Based on Tuning Methods," Applied Mathematics & Information Sciences, Vol.10, Jan. 2016, pp. 343-350, doi:10.18576/amis/100136.

[7] Şeyma Akyürek, Gizem Sezin Özden, Emre Atlas, and Coşku Kasnakoğlu, "Design of a Flight Stabilizer System and Automatic Control Using HIL Test Platform," International Journal of Mechanical Engineering and Robotics Research, Vol. 5, No. 1, Jan. 2016, pp. 77-81, doi: 10.18178/ijmerr.5.1.77-81

[8] [Online] Available at: https://www.mathworks.com/ [Accessed 19 Jan. 2017].

[9] Mansoor Ahsan, Khalid Rafique, and Farrukh Mazhar, "Optimization based tuning of autopilot gains for a Fixed Wing UAV," World Academy of Science, Engineering and Technology, vol. 77, 2013, pp.781-786.

[10] Nathan V. Hoffer, Calvin Coopmans, Austin M. Jensen, and YangQuan Chen, "A Survey and Categorization of Small Low-Cost Unmanned Aerial Vehicle System Identification," Journal of Intelligent and Robotic Systems, vol. 74, April 2014, pp 129–145, doi: 10.1007/s10846-013-9931-6.

[11] Mark B. Tischler and Robert K. Remple, Aircraft and Rotorcraft System Identification Engineering Methods with Flight Test Examples. AIAA education series, 2006.

[12] Downs J., Prentice R., Dalzell S., Besachio A., Ivler C.M., Tischler M.B., and Mansur M.H., "Control system development and flight test experience with the MQ-8B fire scout vertical take-off unmanned aerial vehicle (VTUAV)," American Helicopter Society 63rd Annual Forum. Virginia Beach, VA, 2007.

[13] Parth Kumar and James E. Steck, "System Identification, HIL and Flight Testing of an Adaptive Controller on a Small Scale Unmanned Aircraft," Proc. AIAA Modeling and Simulation Technologies Conference, Jan. 2015, doi:10.2514/6.2015-1803.

[14] Eric Tobias, Mark Tischler, Tom Berger, and Steven G. Hagerott. "Full Flight-Envelope Simulation and Piloted Fidelity Assessment of a Business Jet Using a Model Stitching Architecture," Proc. AIAA Modeling and Simulation Technologies Conference, Jan. 2015, doi:10.2514/6.2015-1594.

[15] Eugene A. Morelli, "Low-Order Equivalent System Identification for the Tu-144LL Supersonic Transport Aircraft," Journal of Guidance, control, and Dynamics, vol. 26, 2003, pp. 354-362, doi:10.2514/2.5053.